NS properties
Phase transitions
Phase diagram
Constraints on realistic EoS

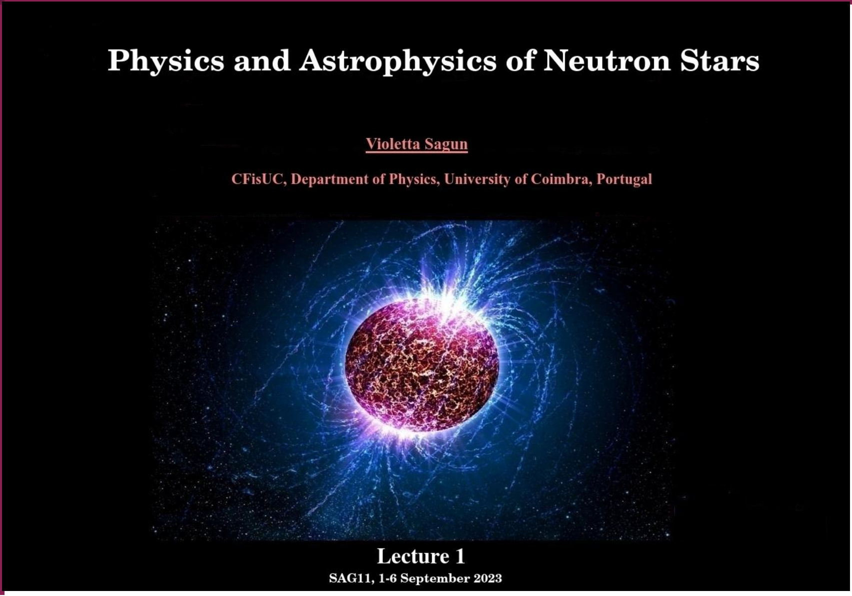

Physics and Astrophysics of Neutron Stars

Violetta Sagun

CFisUC, Department of Physics, University of Coimbra, Portugal

Lecture 1

SAG11, 1-6 September 2023

Neutron star has a size of Lisbon

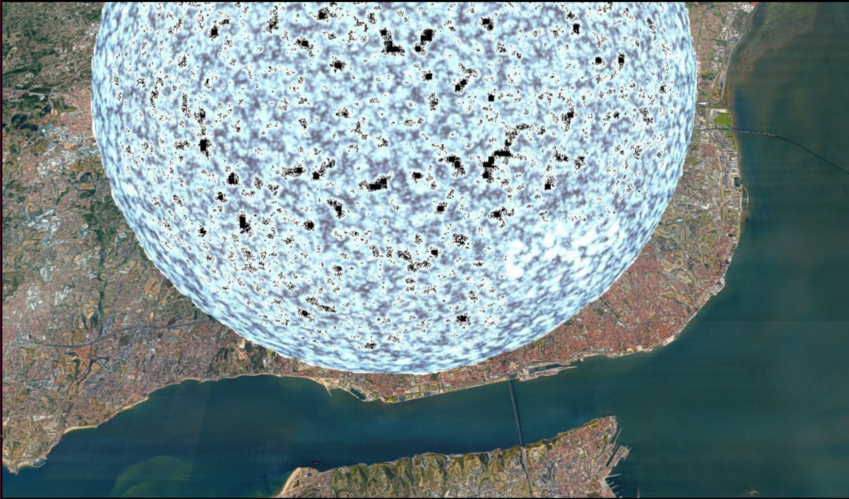

Stellar evolution

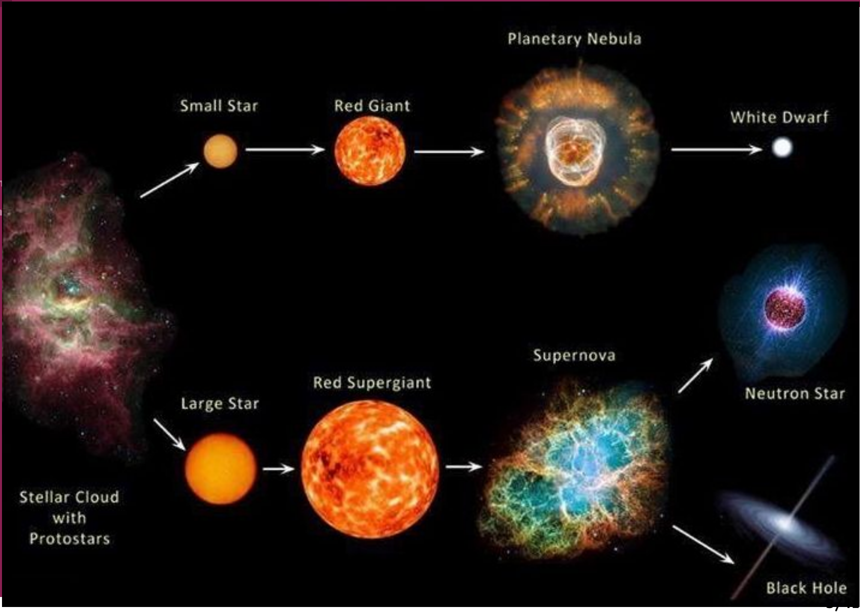

Pulsar - rotating neutron star

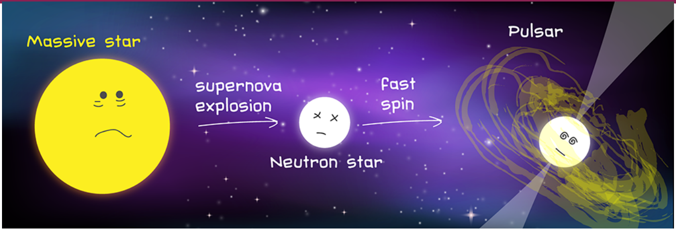

Pulsars can spin up to 1000 times per second!

Neutron star

- the last stage of massive star evolution, produced in core collapse supernova explosion. Usually detected as a pulsar
- the most compact and exotic astrophysical objects in the universe that are accessible by direct observations
- the most extreme objects in terms of the rotation speed, density, radius, magnetic field, etc.

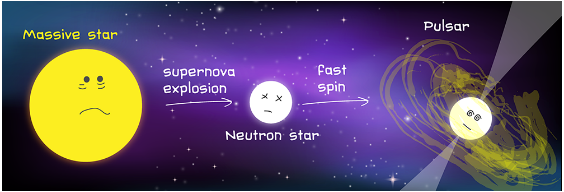

	Neutron star	White dwarf	Sun
$M_{max}(M_\odot)$	2	1.44	1
R (km)	11-12	10^4	$7 \cdot 10^5$
n_c (g/cm^3)	$10^{14} - 10^{15}$	10^7	10^2
rotation speed (s)	$10^{-3} - 1$	100	$2 \cdot 10^6$
B (G)	$10^8 - 10^{16}$	100	1
T (K)	$10^6 - 10^{11}$	10^3	10^5

Outer crust

On the surface $p = 0$ as there is nothing above the crust

NS temperature $T \sim 10^9 K$. The thermal energy is pretty small compared with the Fermi energy, thus the standard NS model uses the zero-temperature approximation, Typical 'excitation energies' $\sim 10^{10} K \simeq MeV$. Thus, NS can be regarded as being in the 'lowest energy state' - the ground state of matter

- Nucleons arranged into Fe^{56} nuclei, the most tightly bound nucleons. Nuclei arranged in a periodic lattice to minimize the energy.
- At density $10^4 g\ cm^{-3}$ atoms become completely ionized.
- When the Fermi energy of the electrons exceeds $\sim 1 MeV$, Fe^{56} is not any more a favoured nucleus due to inverse beta decay.

  $$p + e^- \rightarrow n + \nu \tag{1}$$

  Electrons from the top of the Fermi sea will combine with protons to form neutrons. Neutrinos will escape.
- Due to inverse beta decay nuclei will become more and more neutron rich. Now on Ni^{62} will become more preferable nuclei. It continues until density becomes equal to $4.3\ 10^{11} g\ cm^{-3}$

Binding energies of nuclei

Binding energy per nucleon

n+n, p+p: no binding
d = n+p: 1.1 MeV
α = 2n +2p: 7.1 MeV

$^{8}{}_{4}$Be = 2α: no binding

$^{12}{}_{6}$C: 7.68 MeV
$^{16}{}_{8}$O: 7.98 MeV

$^{56}{}_{26}$Fe: 8.79 MeV
$^{62}{}_{28}$Ni: 8.79 MeV

Isotopes: N,Z
Excited nuclei

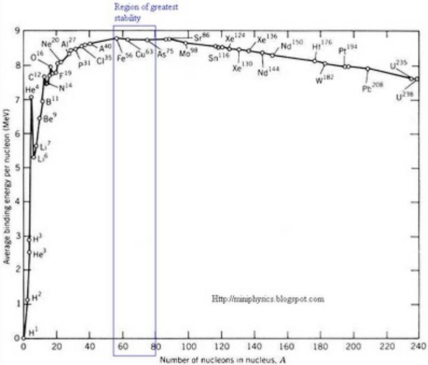

Interior Structure

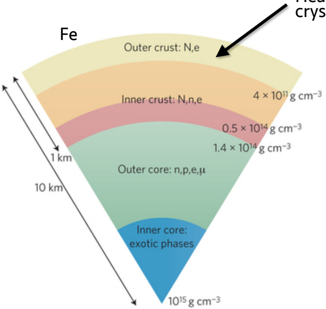

Heavy nuclei in a crystalline e lattice

Credits: Nikolaos Stergiolas

Interior Structure

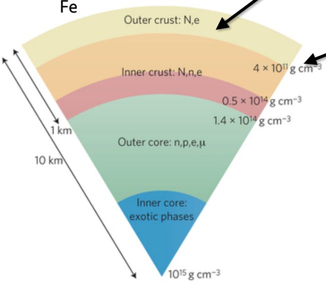

Fe

Heavy nuclei in a crystalline e lattice

Neutron drip

Credits: Nikolaos Stergiolas

Neutron drip line defines the boundary between outer and inner parts of the crust

At density 4.3 $10^{11} g\ cm^{-3}$ nuclei become so neutron rich that neutrons begin to 'drip out' of the nuclei. Inner crust starts to be consist of lattice of exotic nuclei embedded in a sea of neutrons.

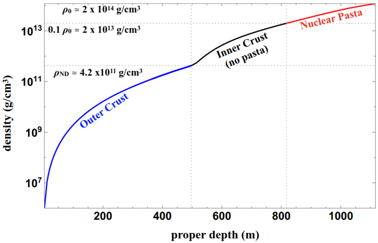

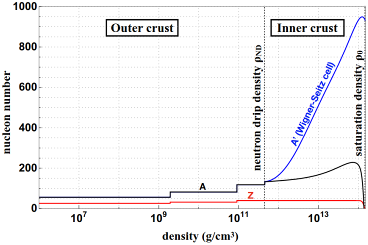

Credits: J. Bramante & N. Raj

Chart of nuclei

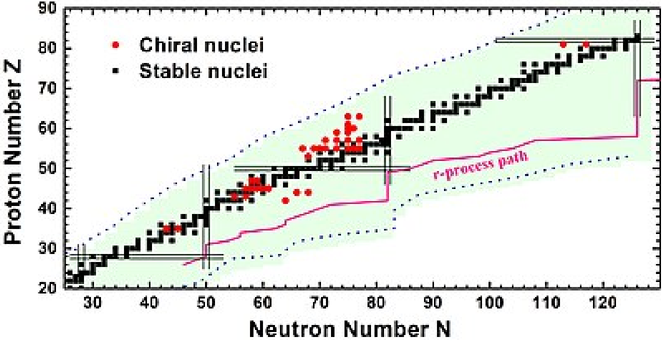

Interior Structure

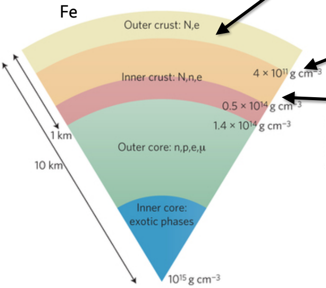

Heavy nuclei in a crystalline e lattice

Neutron drip

N, n, e in β-equilibrium, superfluid n

Credits: Nikolaos Stergiolas

Fluid core

- Above 2.5 $10^{14} g\ cm^{-3}$ the nuclei will 'melt'. A fluid of neutrons, protons and electrons will appear.

- The relative number of neutrons, protons and electrons can be obtained by requiring β equilibrium:

$$n \rightarrow p + e^{-} + \bar{\nu}_e, \quad p + e^{-} \rightarrow n + \nu_e \tag{2}$$

- Chemical equilibrium requires chemical potential of neutrons equals to the sum of chemical potentials of proton and electron.

β equilibrium

Not only neutrons
Matter consists also on
protons, electrons, and further elementary particles

$$\text{neutron mass } m_n = 939.56541 \text{ MeV}$$
$$\text{proton mass } m_p = 938.2708 \text{ MeV}$$
$$\text{electron mass } m_e = 0.511 \text{ MeV}$$

β decay: $n \rightleftharpoons p + e^- + \bar{\nu}_e$
electron antineutrino $\bar{\nu}_e$

chemical equilibrium
$\mu_n = \mu_p + \mu_e + \mu_{\bar{\nu}_e}$
electron antineutrinos escape,
zero density, $\mu_{\bar{\nu}_e} = 0$.
charge neutrality: $n_e = n_p$

Nuclear material constituents

Fermi surfaces:

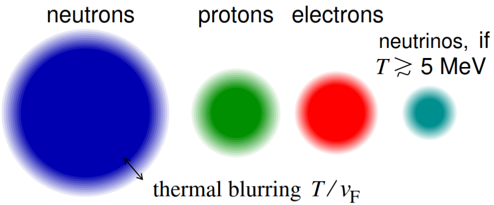

neutrons:	$\sim 90\%$ of baryons	$p_{Fn} \sim 350\,\text{MeV}$
protons:	$\sim 10\%$ of baryons	$p_{Fp} \sim 150\,\text{MeV}$
electrons:	same density as protons	$p_{Fe} = p_{Fp}$
neutrinos:	only present if mfp $\ll 10\,\text{km}$	i.e. when $T \gtrsim 5\,\text{MeV}$

Credits: Mark Alford

"Cold" beta equilibration

At $T \lesssim 1\,\mathrm{MeV}$:

- Fermi surface approximation is valid
- neutrinos escape, so it is the "neutrino-transparent" regime

$$\begin{aligned} n &\rightarrow p + e^- + \bar{\nu}_e \\ p + e^- &\rightarrow n + \nu_e \end{aligned}$$

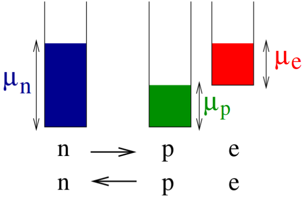

Neutrino energy $\sim T$ is negligible compared to μ_n, μ_p, μ_e.
Beta equilibrium condition is

$$\boxed{\mu_n = \mu_p + \mu_e}$$

- Why does a density change drive the proton fraction out of beta equilibrium?
- What goes wrong with the Fermi Surface approximation as T approaches 1 MeV?

Credits: Mark Alford

Interior of neutron star

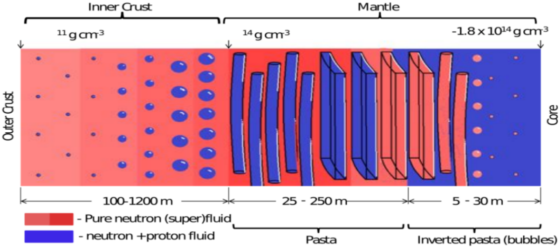

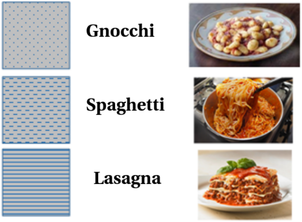

Nuclear pasta configurations produced in Molecular dynamics simulations

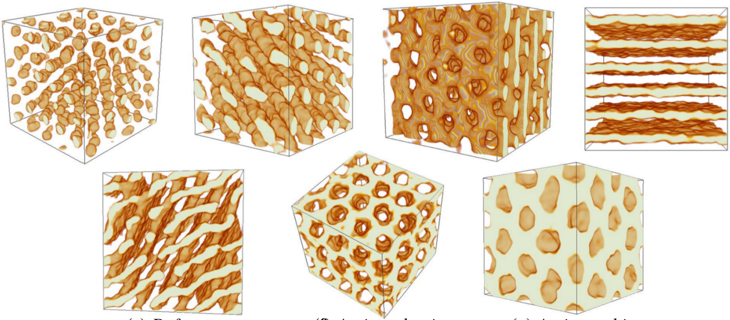

(a) *Gnocchi* **(b)** *Spaghetti* **(c)** *Waffles* **(d)** *Lasagna*

(e) *Defects* **(f)** *Antispaghetti* **(g)** *Antignocchi*

Credits: Horowitz et al., 2015; Schneider et al., 2014, 2013

Interior Structure

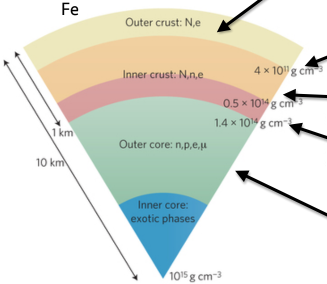

Heavy nuclei in a crystalline e lattice

Neutron drip

N, n, e in β-equilibrium, superfluid n

(possible) mantle with deformed nuclei (“pasta” phase)

superfluid n
superconducting p and e

Credits: Nikolaos Stergiolas

Interior Structure

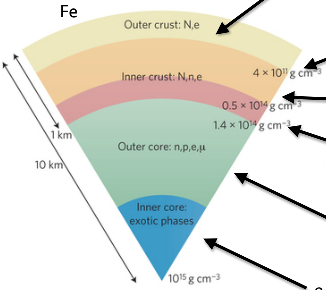

Heavy nuclei in a crystalline e lattice

Neutron drip

N, n, e in β-equilibrium, superfluid n

(possible) mantle with deformed nuclei ("pasta" phase)

superfluid n
superconducting p and e

ρ >> nuclear saturation density $\sim 2 \times 10^{14}$ g/cm^3

Credits: Nikolaos Stergiolas

Different Possible Structures

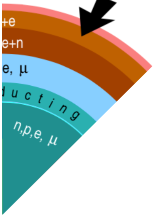

traditional neutron star

[Weber, J. Phys. G **27**, 465 (2001)]

Different Possible Structures

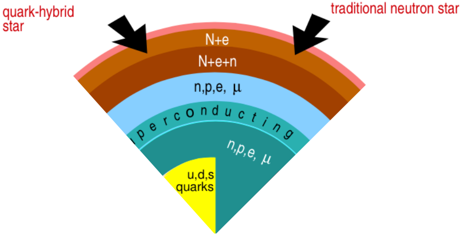

[Weber, J. Phys. G **27**, 465 (2001)]

Different Possible Structures

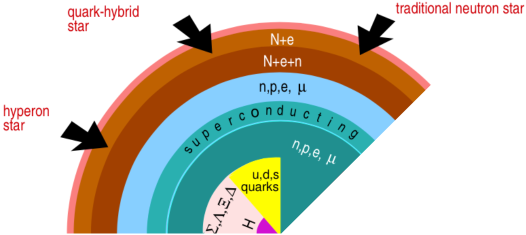

[Weber, J. Phys. G **27**, 465 (2001)]

Different Possible Structures

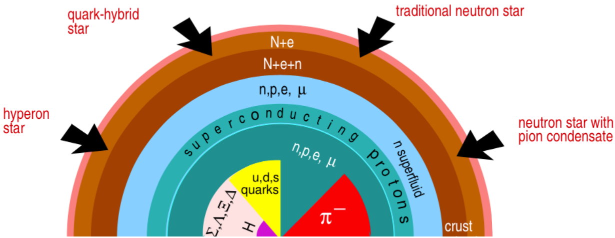

[Weber, J. Phys. G **27**, 465 (2001)]

Different Possible Structures

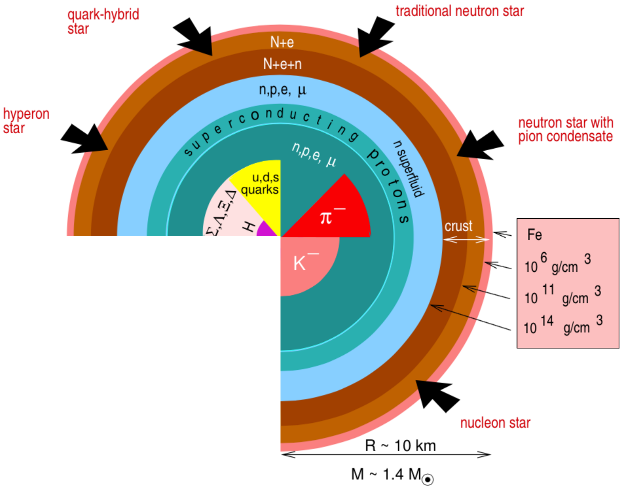

[Weber, J. Phys. G **27**, 465 (2001)]

Different Possible Structures

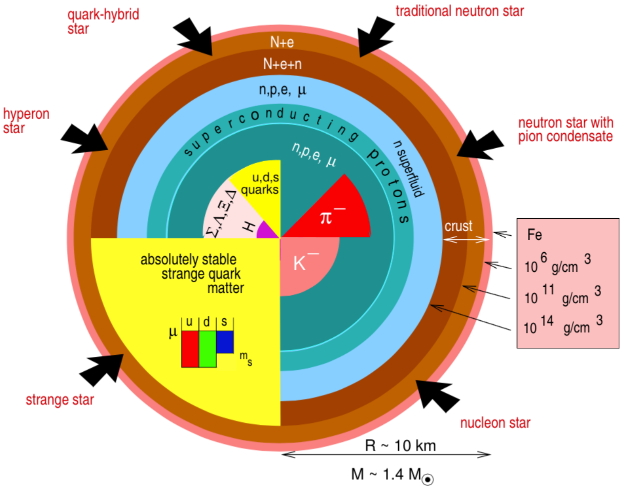

[Weber, J. Phys. G **27**, 465 (2001)]

Phase diagrams - map of matter properties

Phase diagram of water

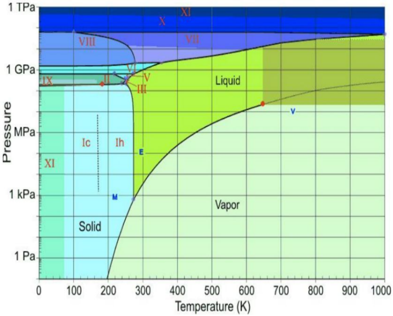

Phase diagram of strongly interacting matter

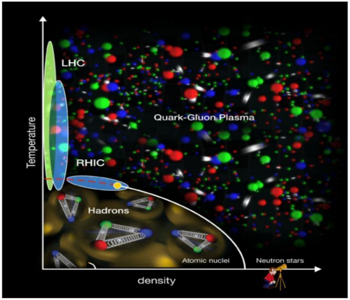

Types of phase transitions

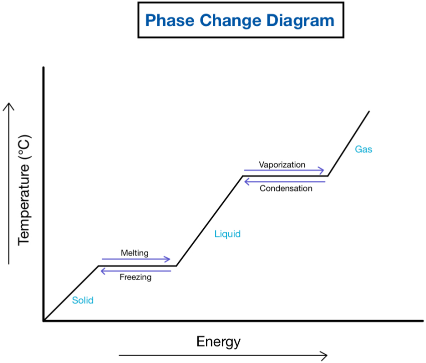

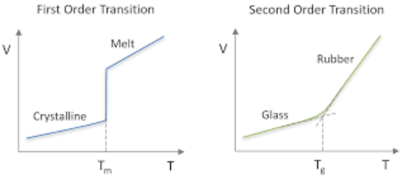

Phase transitions

A phase transition is a change in state from one phase to another

Examples of phase transitions:

- Quantum condensation of bosonic fluids (Bose-Einstein condensation);
- The breaking of symmetries in the laws of physics during the early history of the universe as its temperature cooled;
- Water freezing, evaporation, condensation, sublimation;
- The transition between the ferromagnetic and paramagnetic phases of magnetic materials at the Curie point;
- and many more.

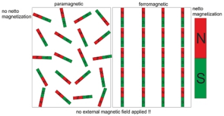

paramagnetic to ferromagnetic phase transition

from zero to non-zero magnetic moment

Phase transition in champagne

Strongly Interacting Matter Phase Diagram

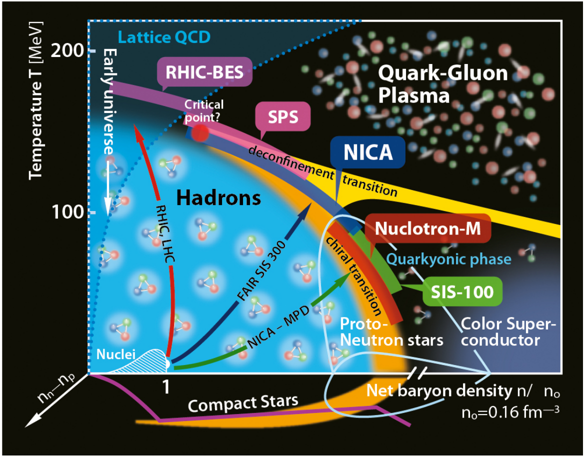

What is Quark-Gluon Plasma?

Proton structure

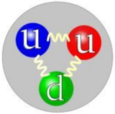

Proton consists of two u and one d quarks
Neutron consists of two d and one u quarks

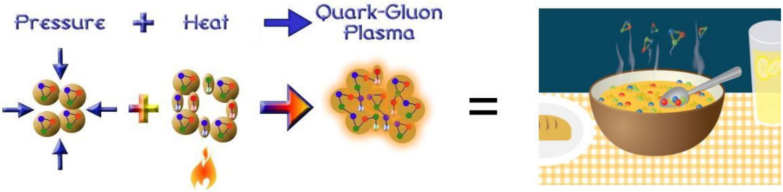

Want to know what is inside? What to do?

To break it apart!!!

Large Hadron Collider (LHC) in CERN

ALICE experiment at the LHC

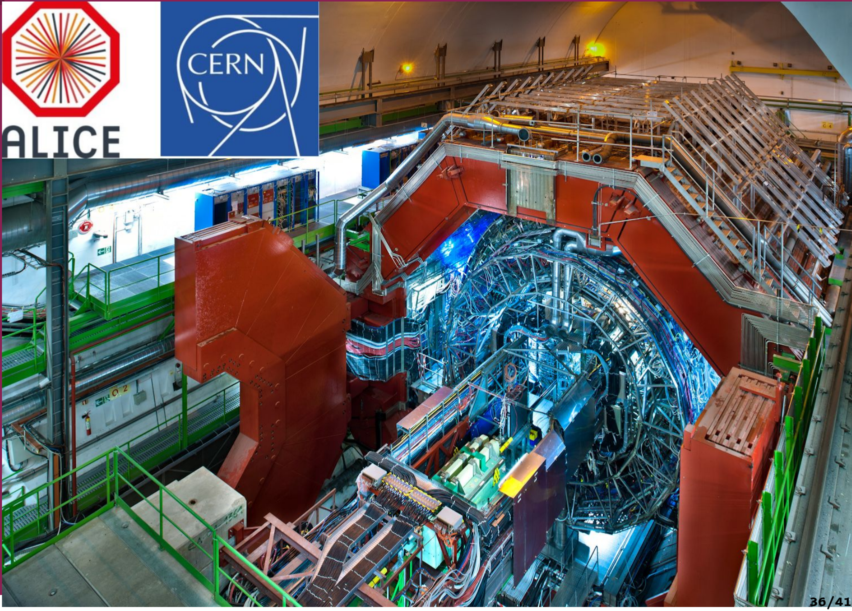

Stages of Heavy-Ion Collisions

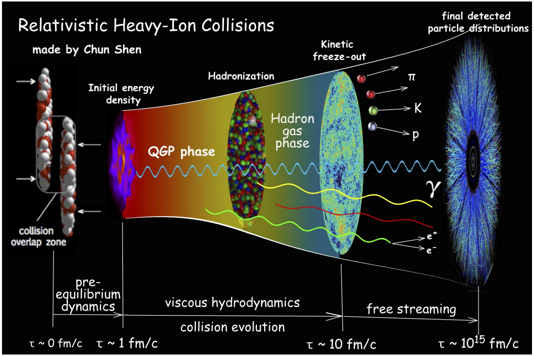

- Non-equilibrium dynamics - the formation of local equilibrium
- The hydrodynamic expansion - local equilibrium
- Hadronisation - formation of full equilibrium
- Hadron freeze-out – full equilibrium, **formation of particle yields**
- Free streaming

Constraints on the EoS

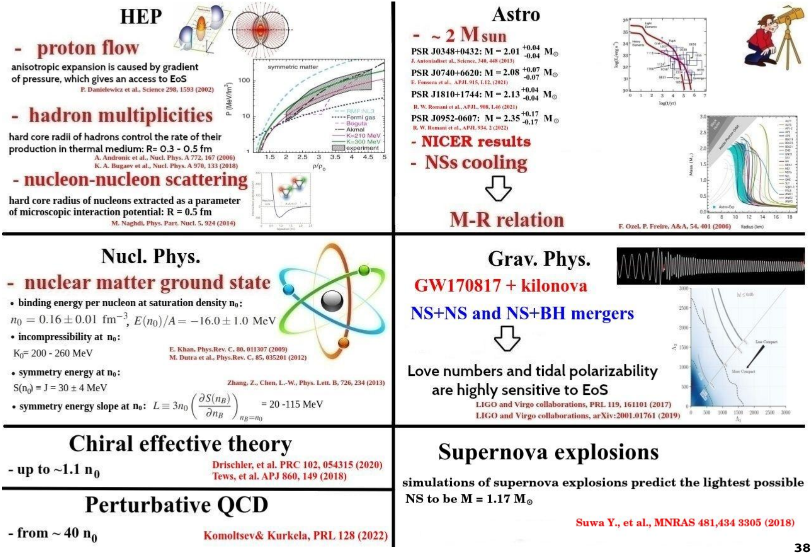

HEP

- **proton flow**

anisotropic expansion is caused by gradient of pressure, which gives an access to EoS

P. Danielewicz et al., Science 298, 1593 (2002)

- **hadron multiplicities**

hard core radii of hadrons control the rate of their production in thermal medium: R= 0.3 - 0.5 fm

A. Andronic et al., Nucl. Phys. A 772, 167 (2006)
K. A. Bugaev et al., Nucl. Phys. A 970, 133 (2018)

- **nucleon-nucleon scattering**

hard core radius of nucleons extracted as a parameter of microscopic interaction potential: R = 0.5 fm

M. Naghdi, Phys. Part. Nucl. 5, 924 (2014)

Astro

- **~ 2 Msun**

PSR J0348+0432: M = 2.01 $^{+0.04}_{-0.04}$ $M_\odot$

J. Antoniadiset al., Science, 340, 448 (2013)

PSR J0740+6620: M = 2.08 $^{+0.07}_{-0.07}$ $M_\odot$

E. Fonseca et al., APJL 915, L12, (2021)

PSR J1810+1744: M = 2.13 $^{+0.04}_{-0.04}$ $M_\odot$

R. W. Romani et al., APJL, 908, L46 (2021)

PSR J0952-0607: M = 2.35 $^{+0.17}_{-0.17}$ $M_\odot$

R. W. Romani et al., APJL 934, 2 (2022)

- **NICER results**
- **NSs cooling**

⇩

M-R relation

F. Ozel, P. Freire, A&A, 54, 401 (2006)

Nucl. Phys.

- **nuclear matter ground state**

- binding energy per nucleon at saturation density n_0:

$n_0 = 0.16 \pm 0.01\ \mathrm{fm}^{-3}$, $E(n_0)/A = -16.0 \pm 1.0$ MeV

- incompressibility at n_0:

K_0= 200 - 260 MeV

E. Khan, Phys.Rev. C, 80, 011307 (2009)
M. Dutra et al., Phys.Rev. C, 85, 035201 (2012)

- symmetry energy at n_0:

$S(n_0) \equiv J = 30 \pm 4$ MeV

Zhang, Z., Chen, L.-W., Phys. Lett. B, 726, 234 (2013)

- symmetry energy slope at n_0: $L \equiv 3n_0 \left(\frac{\partial S(n_B)}{\partial n_B}\right)_{n_B=n_0}$ = 20 -115 MeV

Grav. Phys.

GW170817 + kilonova

NS+NS and NS+BH mergers

⇩

Love numbers and tidal polarizability are highly sensitive to EoS

LIGO and Virgo collaborations, PRL 119, 161101 (2017)
LIGO and Virgo collaborations, arXiv:2001.01761 (2019)

Chiral effective theory

- up to ~1.1 n_0

Drischler, et al. PRC 102, 054315 (2020)
Tews, et al. APJ 860, 149 (2018)

Perturbative QCD

- from ~ 40 n_0

Komoltsev& Kurkela, PRL 128 (2022)

Supernova explosions

simulations of supernova explosions predict the lightest possible NS to be M = 1.17 $M_\odot$

Suwa Y., et al., MNRAS 481,434 3305 (2018)

The nuclear Equation of State (EoS) at T=0

$$\frac{E(n_B,\delta)}{A} = \frac{E(n_B,0)}{A} + S(n_B)\delta^2 + O(\ldots^4)$$

symmetric matter (a)symmetric matter

$$\delta = \frac{n_n - n_p}{n_B}$$

$$n_B = n_n + n_p$$

$$\epsilon = \frac{n_B - n_0}{n_0}$$

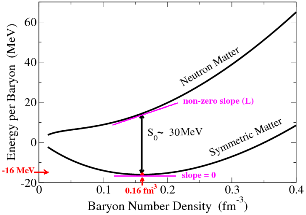

$$\frac{E(n_B,0)}{A} = \frac{E(n_0)}{A} + \frac{1}{18}K_0\epsilon^2$$

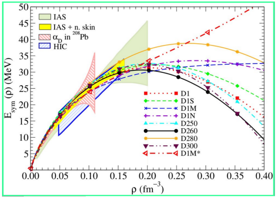

Credits: C. Gonzalez-Boquera

$$S(n_B) = S(n_0) + \frac{1}{3}L\epsilon + \frac{1}{18}K_{sym}\epsilon^2$$

$\frac{E(n_0)}{A} \equiv \frac{E_0}{A} = -16 \pm 1 MeV$ **binding energy per nucleon at saturation density** $n_0 = 0.16 \pm 0.01 fm^{-3}$

$S(n_0) \equiv S_0 \equiv J = 30 \pm 4MeV$

$S(n_0) \equiv \frac{1}{2}\left(\frac{\partial^2 E}{\partial \delta^2}\right)_{\substack{n_B=n_0\\ \delta=0}}$ **symmetry energy at** n_0

$K_0 \equiv 9n_0^2\left(\frac{\partial^2 E}{\partial n_B^2}\right)_{\substack{n_B=n_0\\ \delta=0}} = 200 - 260MeV$ **incompressibility at** n_0

$L \equiv 3n_0\left(\frac{\partial S(n_B)}{\partial n_B}\right)_{\substack{n_B=n_0\\ \delta=0}} = 20 - 115MeV$ **symmetry energy slope at** n_0

EoS ⇔ M-R diagram

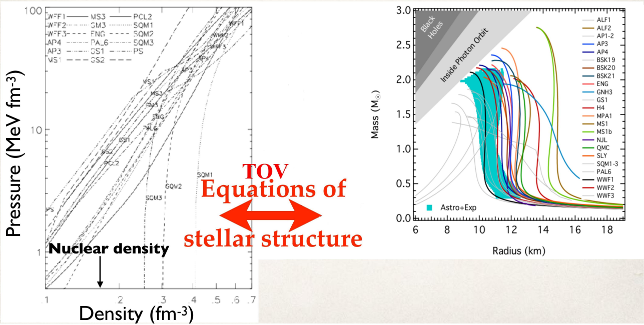

The Tolman-Oppenheimer-Volkoff (TOV) equation constrains the structure of a spherically symmetric body of isotropic material which is in static gravitational equilibrium. The equation is derived by solving the Einstein equations for a general time-invariant, spherically symmetric metric.

$$\frac{dp}{dr} = -(p+\epsilon)\frac{M+4\pi r^3 p}{r(r-2M)}\,, \tag{3}$$

$$\frac{dM}{dr} = 4\pi\epsilon r^2\,, \tag{4}$$

TASK: Derive the TOV Eq.

Mass-Radius diagram

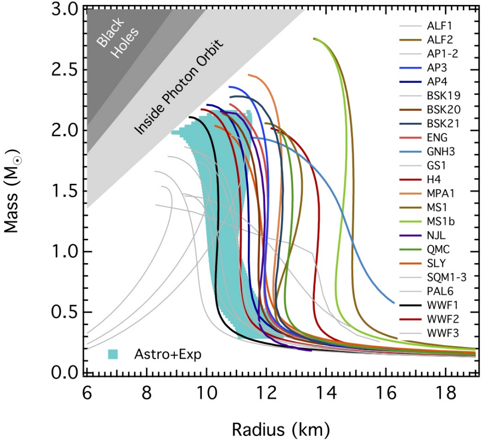

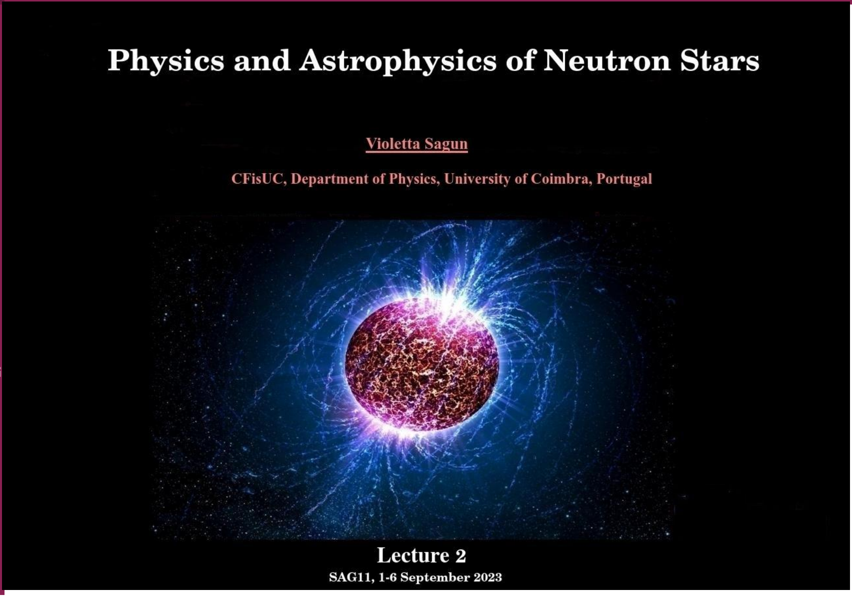

Physics and Astrophysics of Neutron Stars

Violetta Sagun

CFisUC, Department of Physics, University of Coimbra, Portugal

Lecture 2

SAG11, 1-6 September 2023

Equation of state (EoS) $\Longleftrightarrow$ Mass-Radius diagram

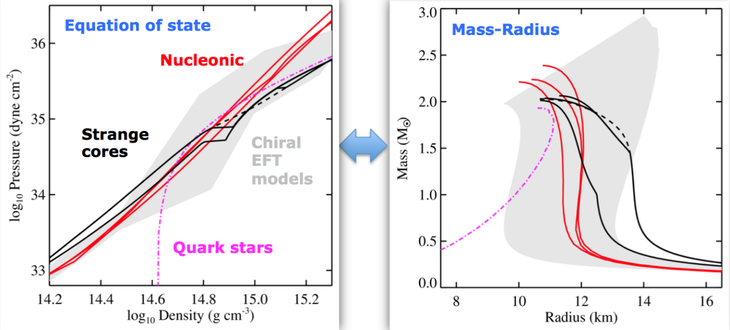

Watts et al. 2015 SKA Science Book

EoS is an input to the Tolman-Oppenheimer-Volkoff (TOV) equation

$$\frac{dp}{dr} = -\frac{(\epsilon + p)(M + 4\pi r^3 p)}{r^2\,(1 - 2M/r)}, \tag{1}$$

Third family of compact stars

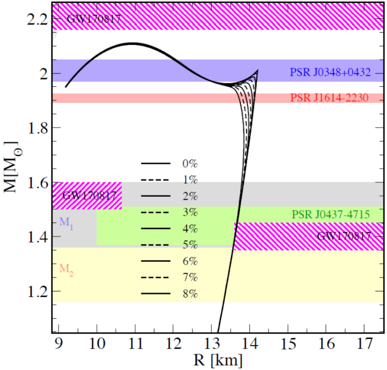

Credits: David Alvarez-Castillo, David Blaschke, arXiv:1807.03258 [nucl-th]

Hybrid Stars

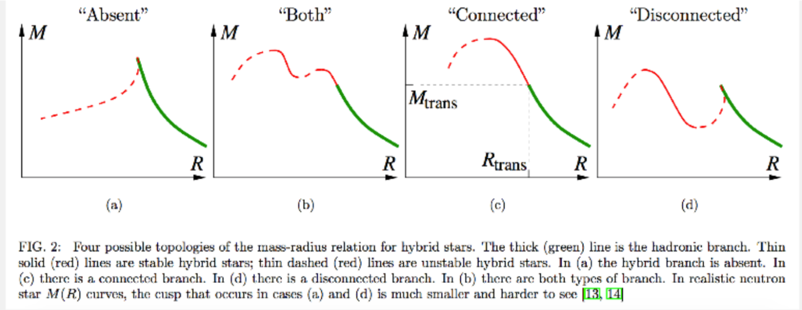

FIG. 2: Four possible topologies of the mass-radius relation for hybrid stars. The thick (green) line is the hadronic branch. Thin solid (red) lines are stable hybrid stars; thin dashed (red) lines are unstable hybrid stars. In (a) the hybrid branch is absent. In (c) there is a connected branch. In (d) there is a disconnected branch. In (b) there are both types of branch. In realistic neutron star $M(R)$ curves, the cusp that occurs in cases (a) and (d) is much smaller and harder to see [13, 14]

Alford, Han, and Prakash (2013)

Strange stars

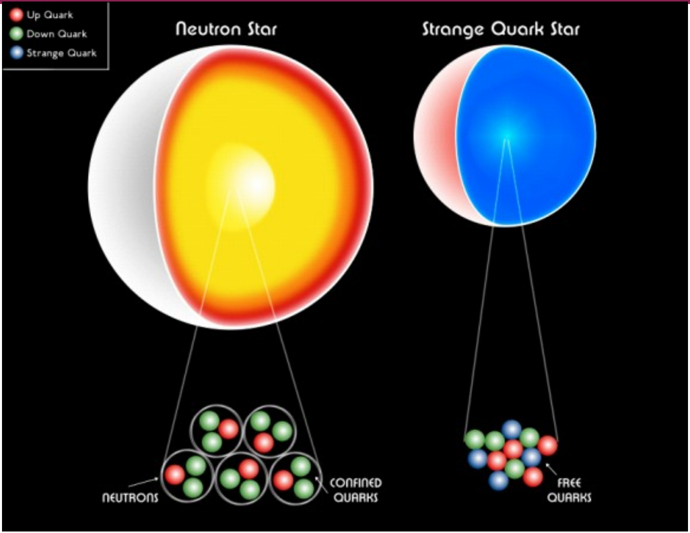

Strange star M-R diagram

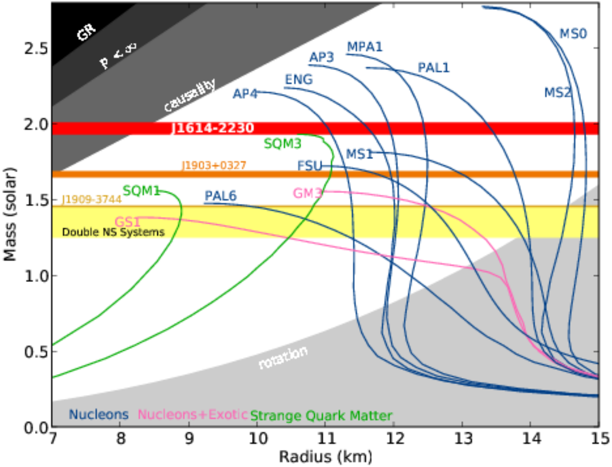

NS masses

- **> 2500 pulsars known**

About 90% of radio pulsars are isolated → Mass cannot be measured

The remaining 250 pulsars are located in binary systems → info on mass

PSR J0348+0432
M=(2.01 ± 0.04) Msun (Antoniadis et al '13)

PSR J0740+6620
M=$2.14^{+0.20}_{-0.18}$ Msun (Cromartie et al. '19)

- **High precision determined masses:**
Hulse-Taylor pulsar
M=1.4414 ± 0.0002 Msun
Hulse-Taylor Nobel Prize 1994

Ozel & Freire 2016

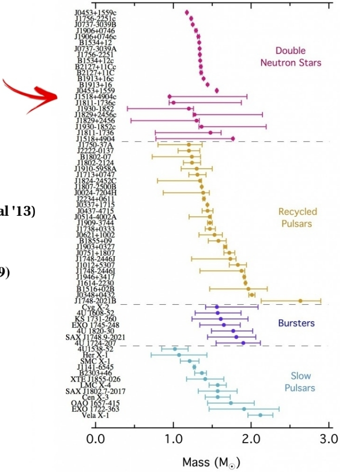

- Hulse-Taylor binary system (PSR B1913+16) is the first system for which reliable mass measurements were made. Consist of pulsar and an NS.
1993 Nobel Prize in Physics "for the discovery of a new type of pulsar, a discovery that has opened up new possibilities for the study of gravitation".

Neutron star masses

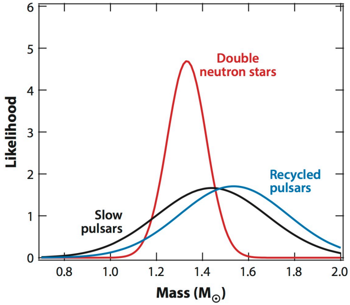

inferred mass distributions
for the different populations of neutron stars.

F. Ozel and P. Freire, Annu. Rev. Astron. Astrophys. **54**, 401 (2016)

M and R measurements

4 NSs with mass above $2M_\odot$

- PSR J0348+0432: $M = 2.01^{+0.04}_{-0.04} M_\odot$ (Antoniadis+ 2013)
- PSR J0740+6620: $M = 2.08^{+0.07}_{-0.07} M_\odot$ (Fonseca+ 2021)
- PSR J1810+1744: $M = 2.13^{+0.04}_{-0.04} M_\odot$ (Romani+ 2021)
- PSR J0952-0607: $M = 2.35^{+0.17}_{-0.17} M_\odot$ (Romani+ 2022)

Radius measurements have big uncertainties that are related to the modelling of the atmosphere composition

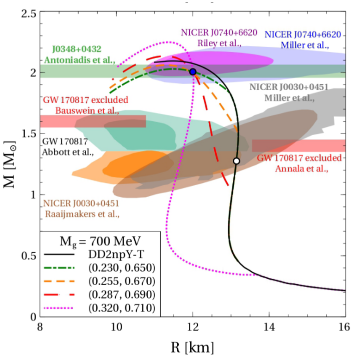

Ivanytskyi&Blaschke 2022

Binary system

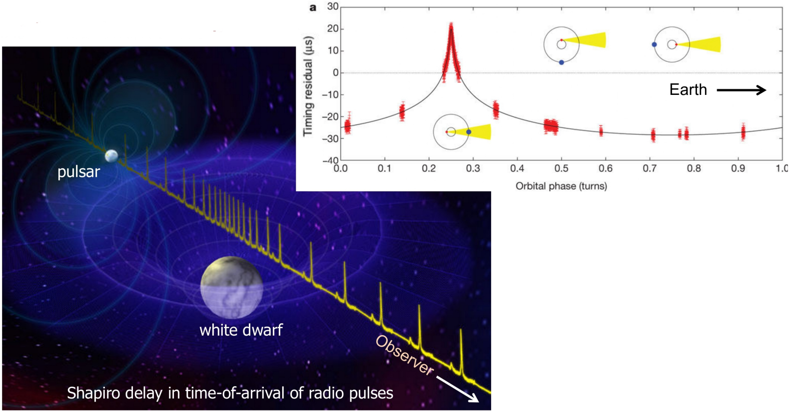

Example

Demorest et al. (2010)

Pulsar mass: 1.97±0.04 M_{sun}
White dwarf mass: 0.500±0.006 M_{sun}
Orbital period: 8.69 days
Pulsar spin period: 3.15 ms

Neutron Star Interior Composition ExploreR (NICER)

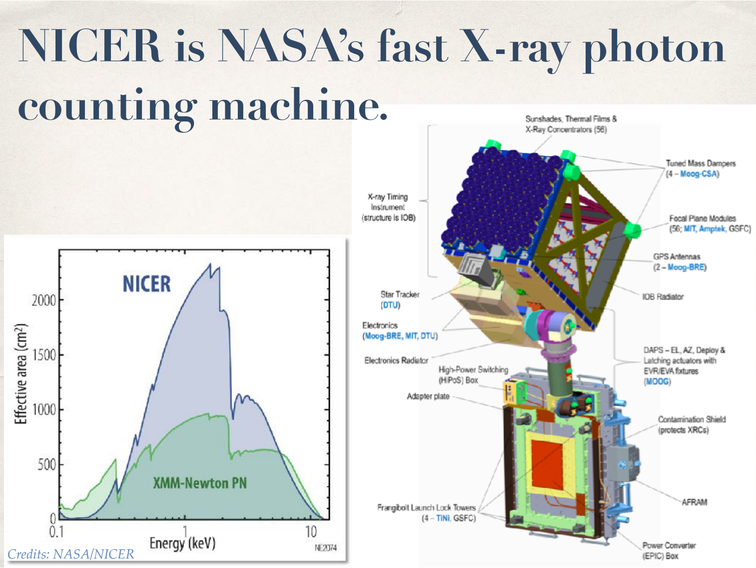

NICER is NASA's fast X-ray photon counting machine.

Credits: NASA/NICER

Credits: Sebastien Guillot

The pulsed emission caused by hot spots on a rotating neutron star can help measure the compactness.

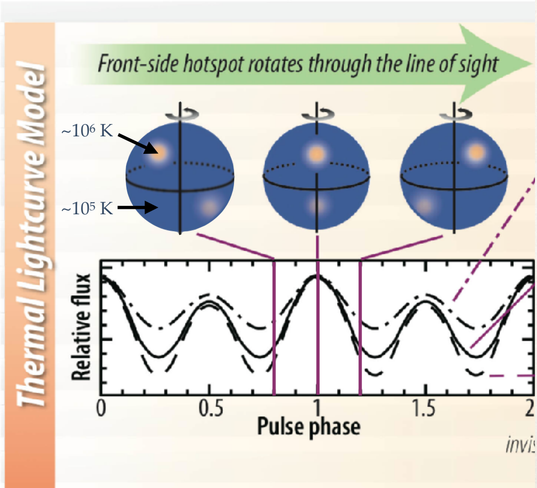

NICER results

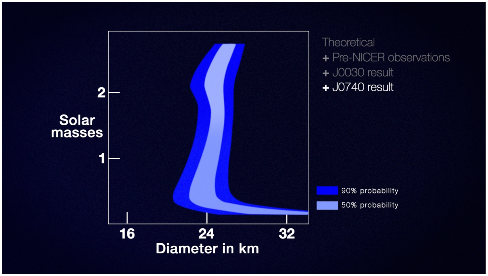

Credits: NASA

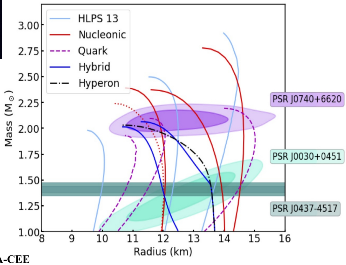

Credits: JINA-CEE

Double pulsar system

- PSR J0737-3039 (PSR J0737-3039A (1.337 $M_\odot$) & PSR J0737-3039B (1.250 $M_\odot$)) is the only known system containing two pulsars – thus a 'double pulsar' system.
- The orbit has decayed since the binary system was initially discovered, in precise agreement with the loss of energy due to gravitational waves described by Einstein's general theory of relativity.

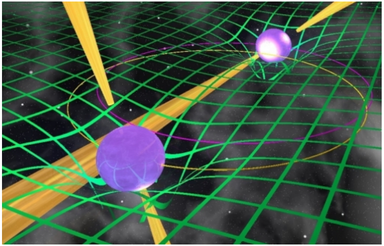

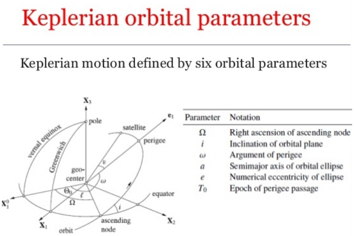

Keplerian orbital parameters

Keplerian motion defined by six orbital parameters

Parameter	Notation
Ω	Right ascension of ascending node
i	Inclination of orbital plane
ω	Argument of perigee
a	Semimajor axis of orbital ellipse
e	Numerical eccentricity of ellipse
T_0	Epoch of perigee passage

Post-Keplerian parameters

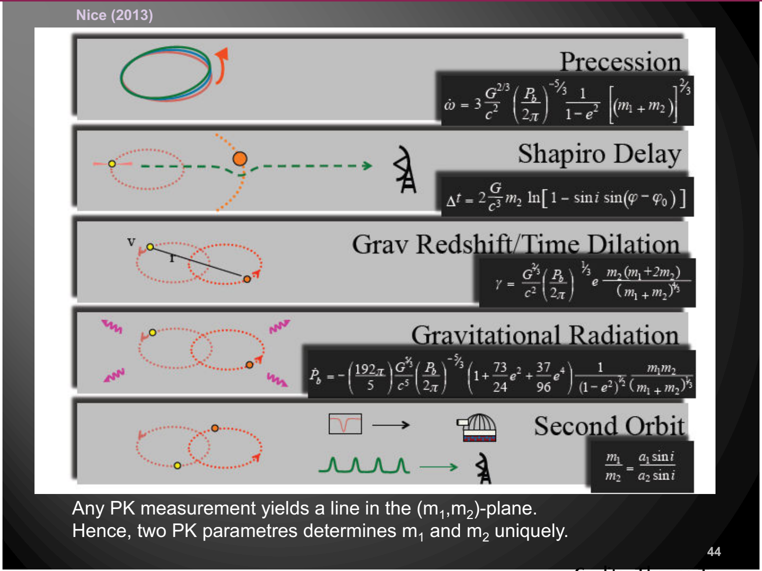

Nice (2013)

Precession

$$\dot{\omega} = 3\frac{G^{2/3}}{c^2}\left(\frac{P_b}{2\pi}\right)^{-5/3}\frac{1}{1-e^2}\left[(m_1+m_2)\right]^{2/3}$$

Shapiro Delay

$$\Delta t = 2\frac{G}{c^3}m_2\ \ln[\,1-\sin i\ \sin(\varphi-\varphi_0)\,]$$

Grav Redshift/Time Dilation

$$\gamma = \frac{G^{2/3}}{c^2}\left(\frac{P_b}{2\pi}\right)^{1/3} e\,\frac{m_2(m_1+2m_2)}{(m_1+m_2)^{4/3}}$$

Gravitational Radiation

$$\dot{P}_b = -\left(\frac{192\pi}{5}\right)\frac{G^{5/3}}{c^5}\left(\frac{P_b}{2\pi}\right)^{-5/3}\left(1+\frac{73}{24}e^2+\frac{37}{96}e^4\right)\frac{1}{(1-e^2)^{7/2}}\frac{m_1 m_2}{(m_1+m_2)^{1/3}}$$

Second Orbit

$$\frac{m_1}{m_2} = \frac{a_1\sin i}{a_2\sin i}$$

Any PK measurement yields a line in the (m_1,m_2)-plane.
Hence, two PK parametres determines m_1 and m_2 uniquely.

44

Credits: Thomas Tauris

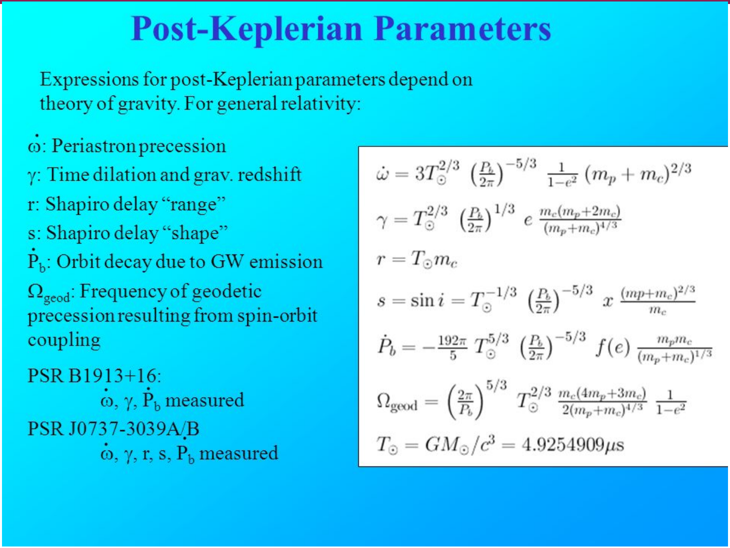

Post-Keplerian Parameters

Expressions for post-Keplerian parameters depend on theory of gravity. For general relativity:

$\dot{\omega}$: Periastron precession

γ: Time dilation and grav. redshift

r: Shapiro delay "range"

s: Shapiro delay "shape"

$\dot{P}_b$: Orbit decay due to GW emission

Ω_{geod}: Frequency of geodetic precession resulting from spin-orbit coupling

PSR B1913+16:

$\dot{\omega}$, γ, $\dot{P}_b$ measured

PSR J0737-3039A/B

$\dot{\omega}$, γ, r, s, $\dot{P}_b$ measured

$$\dot{\omega} = 3T_{\odot}^{2/3}\ \left(\tfrac{P_b}{2\pi}\right)^{-5/3}\ \tfrac{1}{1-e^2}\,(m_p+m_c)^{2/3}$$

$$\gamma = T_{\odot}^{2/3}\ \left(\tfrac{P_b}{2\pi}\right)^{1/3}\ e\,\tfrac{m_c(m_p+2m_c)}{(m_p+m_c)^{4/3}}$$

$$r = T_{\odot} m_c$$

$$s = \sin i = T_{\odot}^{-1/3}\ \left(\tfrac{P_b}{2\pi}\right)^{-5/3}\ x\,\tfrac{(mp+m_c)^{2/3}}{m_c}$$

$$\dot{P}_b = -\tfrac{192\pi}{5}\,T_{\odot}^{5/3}\ \left(\tfrac{P_b}{2\pi}\right)^{-5/3}\ f(e)\,\tfrac{m_p m_c}{(m_p+m_c)^{1/3}}$$

$$\Omega_{\rm geod} = \left(\frac{2\pi}{P_b}\right)^{5/3}\ T_{\odot}^{2/3}\,\tfrac{m_c(4m_p+3m_c)}{2(m_p+m_c)^{4/3}}\,\tfrac{1}{1-e^2}$$

$$T_{\odot} = GM_{\odot}/c^3 = 4.9254909\mu{\rm s}$$

Credits: Scuola nazionale de Astrofisica Radio Pulsars

Confirmation of GR

Mass-mass diagram for the J0737-3039 system. All lines meet at a single point in the diagram, i.e., GR passes the tests posed by these four distinct constraints.

The orbital decay due to the emission of gravitational waves has been measured for six DNS systems: PSR B1913+16, J0737-3039A/B, B1534+12, J1756-2251, J1906+0746 and B2127+11C.

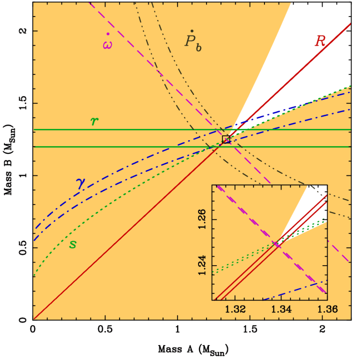

Credits: Kramer et al. 2006

Millisecond pulsars

- Millisecond pulsars (MSPs) refers to pulsars with spin periods in the range $1.39 < P < 20$ ms and $\dot{P} < 10^{-19}$.
- These systems have been heavily recycled by a long-lived accretion phase in a low-mass X-ray binary (LMXB).
- $\sim 20\%$ are isolated, most of the remaining objects have white dwarf companions and very small orbital eccentricities.
- The fast (and very stable) rotation of MSPs makes their timing significantly more precise than for the pulsars in DNSs. However, their low orbital eccentricities pose a problem for mass determination (and tests of GR), since, in these cases, the PK parameters $\dot{w}$ and γ cannot be measured accurately.
- MSPs in globular clusters (GCs) have gravitational interactions with nearby stars that, with time, can make an initially circular orbit acquire a substantial eccentricity $\Longrightarrow$ possible to measure $\dot{w}$ and total mass.

Generic Evolution of Pulsars

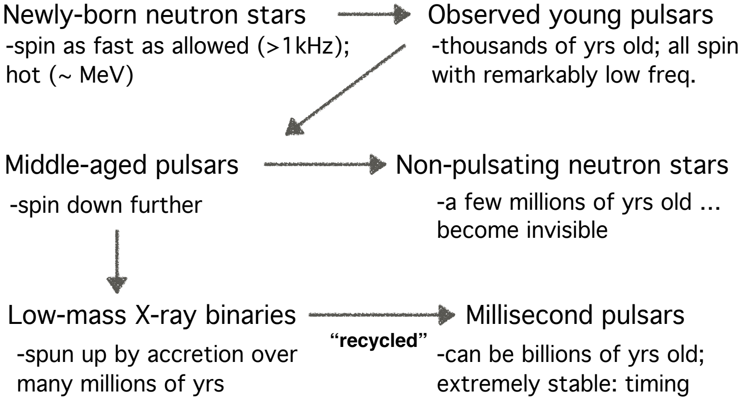

Newly-born neutron stars

-spin as fast as allowed (>1kHz); hot (~ MeV)

Observed young pulsars

-thousands of yrs old; all spin with remarkably low freq.

Middle-aged pulsars

-spin down further

Non-pulsating neutron stars

-a few millions of yrs old ... become invisible

Low-mass X-ray binaries

-spun up by accretion over many millions of yrs

"recycled"

Millisecond pulsars

-can be billions of yrs old; extremely stable: timing

Credits: Sophia Han

$P - \dot{P}$ diagram

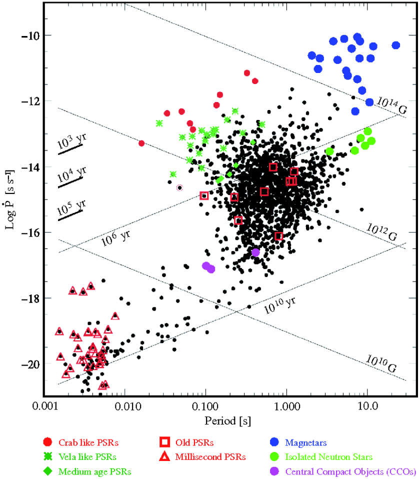

Credits: W.Becker, M.G. Bernhardt, A. Jessner, arXiv:1305.4842

International Pulsar Timing Array

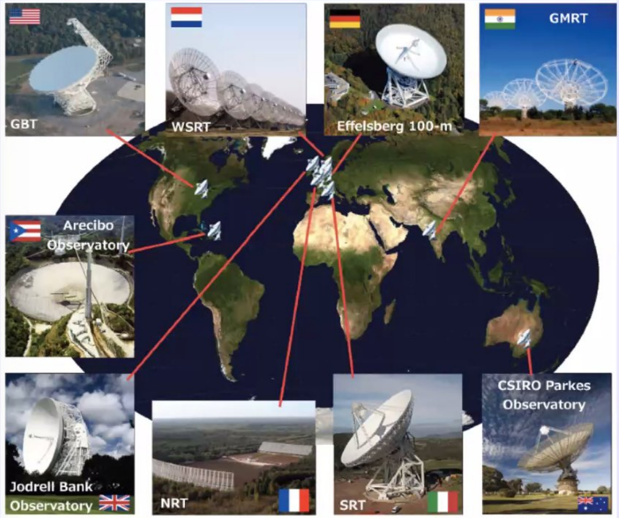

EPTA

NANOGrav

PPTA

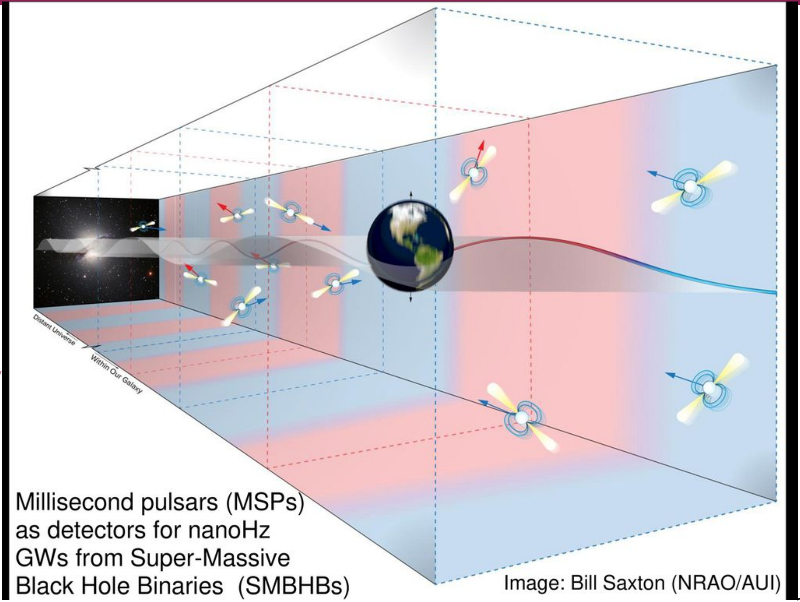

Millisecond pulsars (MSPs) as detectors for nanoHz GWs from Super-Massive Black Hole Binaries (SMBHBs)

Image: Bill Saxton (NRAO/AUI)

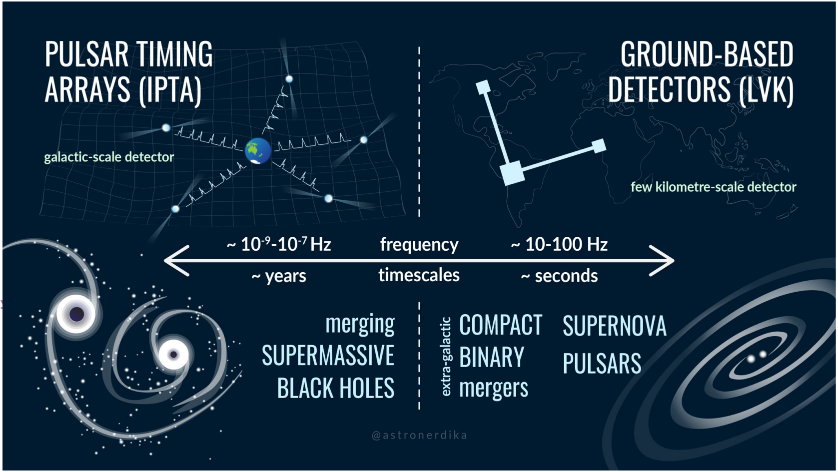
PULSAR TIMING ARRAYS (IPTA)
galactic-scale detector
GROUND-BASED DETECTORS (LVK)
few kilometre-scale detector
~ 10^{-9}-10^{-7} Hz
frequency
~ 10-100 Hz
~ years
timescales
~ seconds
merging SUPERMASSIVE BLACK HOLES
extra-galactic
COMPACT BINARY mergers
SUPERNOVA
PULSARS
@astronerdika

First results

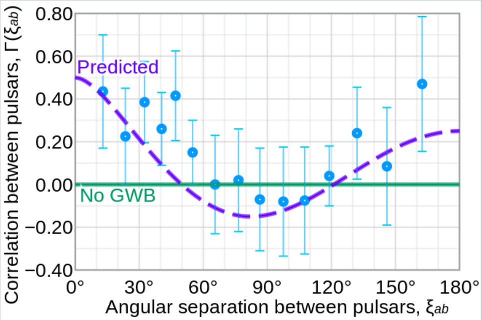

Plot of correlation between pulsars observed by NANOGrav (2023) vs angular separation between pulsars, compared with a theoretical model (dashed purple, or *Hellings-Downs* curve) and if there were no gravitational wave background (solid green)

$P - \dot{P}$ diagram

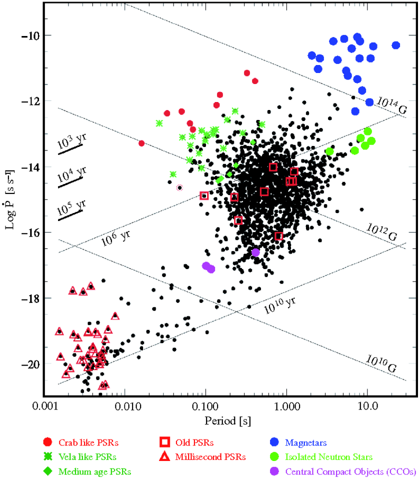

Credits: W.Becker, M.G. Bernhardt, A. Jessner, arXiv:1305.4842

Magnetars (magnetic star)

- Ultra-strong magnetic field $\sim 10^{14} - 10^{15}$ gauss.
  For comparison: magnetic field strength of Earth ~ 0.5 gauss, normal star ~ 100 gauss, Sunspots ~ 3000 gauss, pulsars $\sim 10^{12}$ gauss.
- Young NSs.
- Sources of the soft γ repeaters (SGR) and anomalous X-ray pulsars powered by the decay of the magnetic field.

  SGR is an astronomical object which emits large bursts of γ -rays and X-rays at irregular intervals.
- Ultra-strong NS field decay, causing extreme heating of crust $\Longrightarrow$ high X-ray luminosity.
- Starquakes triggered on the surface of the magnetar disturb the magnetic field leading to extremely powerful γ-ray flare emissions.

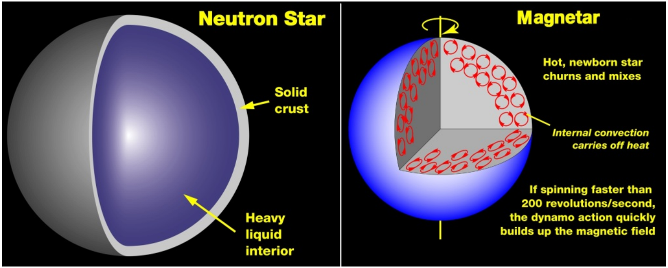

Magnetars

- During initial formation of NS, rapid spin of core can produce magnetic fields as high as 10^{15-16} G - most NSs do no spin fast upon formation, prohibiting this dynamo from operating; more "typical"pulsar fields result.

Credits: Patric Slane

Strongest magnetic field that could possibly be contained in a NS

$$\frac{B_{max}^2}{8\pi} \sim P \sim \frac{GM^2}{R^4} \implies B_{max} \sim 4 \cdot 10^{18} G \tag{2}$$

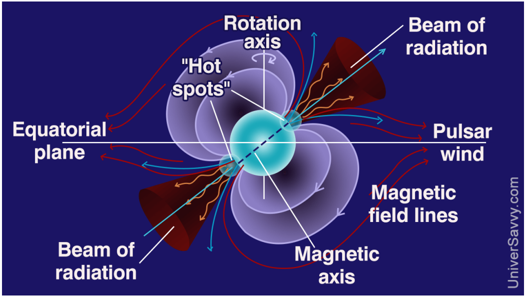

Glitches

A glitch is a sudden increase in the rotational frequency of a rotation-powered pulsar. Following a glitch is a period of gradual recovery where the observed periodicity slows to a period close to that observed before the glitch. These gradual recovery periods have been observed to last from days to years. Currently, only multiple glitches of the Crab and Vela pulsars have been observed and studied extensively.)

Explanation: Glitches are thought to be the result of a rapid transfer of angular momentum between this inner superfluid and the outer crust, to which the NS magnetosphere is attached and whose radiation we observe.
The process leading to a glitch is believed to be from the interior of the NS, rather than from the magnetosphere which causes the spin down. This is because the structure of pulses observed during glitch events remains unchanged.

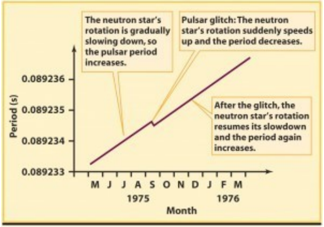

Credits: S.A. Abdullah, M.M. Yaseen

QCD phase diagram

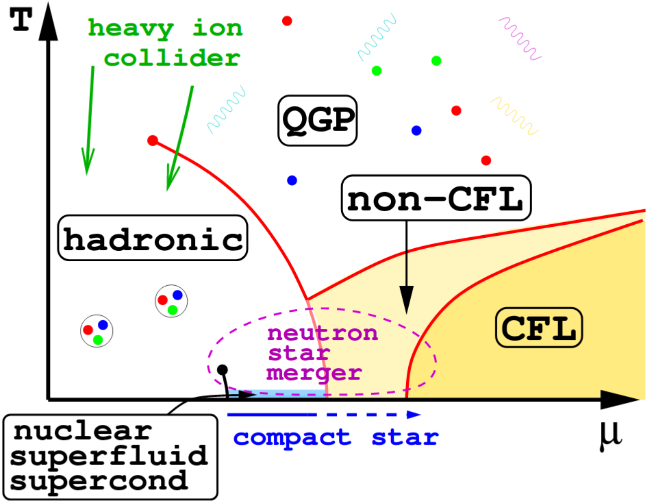

Cooper pairing in NSs

The Cooper pairing appears as a result of the attraction of particles with the anti-parallel momenta,which is expected to occur, at low enough temperature, in any degenerate system of fermions in which there is an attractive interaction between particles whose momenta lie close to the Fermi surface

---

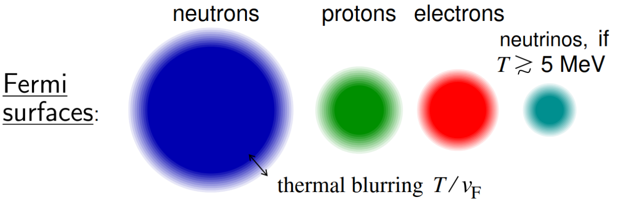

neutrons:	$\sim 90\%$ of baryons	$p_{Fn} \sim 350$ MeV
protons:	$\sim 10\%$ of baryons	$p_{Fp} \sim 150$ MeV
electrons:	same density as protons	$p_{Fe} = p_{Fp}$
neutrinos:	only present if mfp $\ll 10$ km	i.e. when $T \gtrsim 5$ MeV

Credits: Mark Alford

Term symbols

$^{2S+1}L_J$

S = total spin quantum number
2S+1 = multiplicity(singlet, doublet, triplet, etc.)
L = total orbital quantum number
J = total angular momentum quantum number

L	**0**	**1**	**2**	**3**	**4**
symbol	**S**	**P**	**D**	**F**	**G**

Example:

$s_1, s_2,\ldots \to S$
$l_1, l_2,\ldots \to L$
$S, L \to J$

=>

$s_1=+1/2 \quad s_2=-1/2 \Rightarrow S=0$ - singlet state
$s_1=+1/2 \quad s_2=+1/2 \Rightarrow S=1$ - triplet state

$^{2*0+1}S_0 = {}^{1}S_0 \qquad {}^{2*1+1}P_2 = {}^{3}P_2$

Pairing in the quark core

Spin-zero pairings

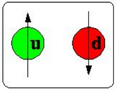

2-flavor SC (2SC)
Bailin, Love (1984)

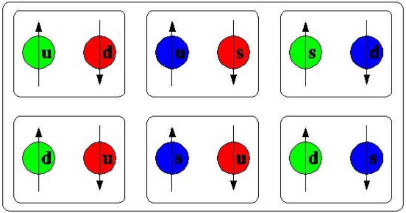

Color-flavor-locking (CFL)
Alford, Rajagopal, Wilczek (1984)

Credits: Qun Wang

Lecture Tomorrow: Multi-Messenger Astrophysics

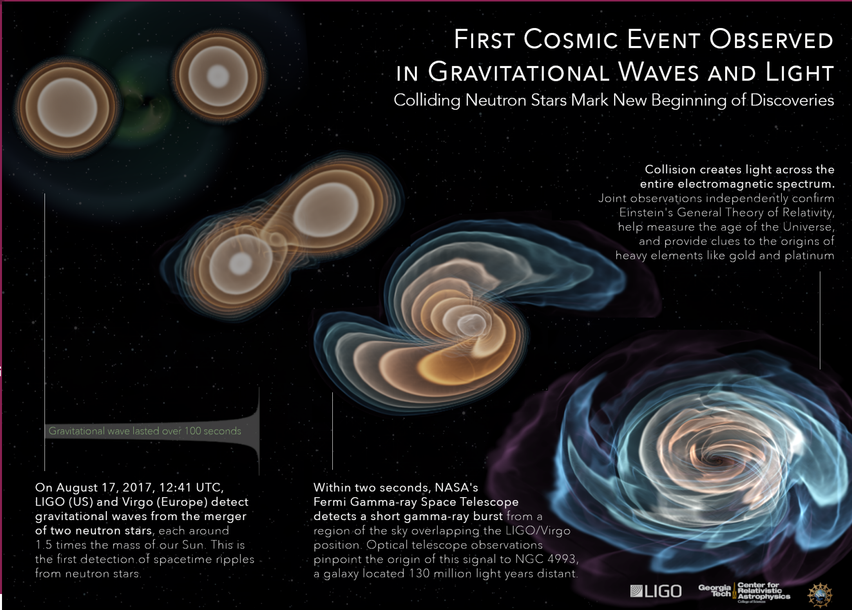

First Cosmic Event Observed in Gravitational Waves and Light

Colliding Neutron Stars Mark New Beginning of Discoveries

Collision creates light across the entire electromagnetic spectrum. Joint observations independently confirm Einstein's General Theory of Relativity, help measure the age of the Universe, and provide clues to the origins of heavy elements like gold and platinum

On August 17, 2017, 12:41 UTC, LIGO (US) and Virgo (Europe) detect gravitational waves from the merger of two neutron stars, each around 1.5 times the mass of our Sun. This is the first detection of spacetime ripples from neutron stars.

Within two seconds, NASA's Fermi Gamma-ray Space Telescope detects a short gamma-ray burst from a region of the sky overlapping the LIGO/Virgo position. Optical telescope observations pinpoint the origin of this signal to NGC 4993, a galaxy located 130 million light years distant.